

KING SAUD UNIVERISTY  
COLLEGE OF ENGINEERING  
**RESEARCH CENTER**

*Final Research Report No. 32/428*

**Achieving Desired Properties Of The Polyethylene Grade Via Optimal  
Control Of The Process Feed**

By

Dr. Mohammad Al-haj Ali  
Dr. Emad Ali

1429 H  
2008 G

## TABLE OF CONTENTS

### Contents

LIST OF TABLES .....	iii
LIST OF FIGURES .....	iv
ACKNOWLEDGMENT .....	v
ABSTRACT .....	vii
SUMMARY .....	1
1. INTRODUCTION .....	3
2. THE PROCESS MODEL .....	5
2.1 Plant Operating Condition .....	7
2.2 The Polymer Properties Model .....	9
3. THE ON-LINE NLMPC ALGORITHM .....	11
4. RESULTS .....	12
4.1 Effect of Hydrogen Feed Flow Rate .....	14
4.2 Effect of Monomer And Hydrogen Feed Flow Rates .....	17
4.3 Optimal Step Changes .....	20
4.4 Online Optimization .....	25
5. CONCLUSIONS .....	27
6. NOMENCLATURE .....	28
7. REFERENCES .....	30

## LIST OF TABLES

Table 1: steady state operating condition .....	9
Table 2: process parameters .....	9

## LIST OF FIGURES

- Figure 1: schematic of the polyethylene reactor 7
- Figure 2: Process outputs at the normal operating condition 13
- Figure 3: The polymer properties and the controlled process variables at the normal operating condition 13
- Figure 4: Process inputs and the molecular weight distribution at the normal operating condition 14
- Figure 5: Process Responses for Hydrogen up-down Step changes 15
- Figure 6: Molecular weight distribution for hydrogen up-down step changes 16
- Figure 7: Process Response to down-up changes in the hydrogen fed flow rate 16
- Figure 8: Molecular weight distribution due to down-up changes in the hydrogen feed flow rate 17
- Figure 9: Process response to simultaneous changes in the hydrogen and monomer flow rates towards higher X. 18
- Figure 10: Molecular weight distribution due to simultaneous changes in the hydrogen and monomer flow rates towards higher X; solid: start of 1<sup>st</sup> step (normal operating condition), dotted: end of 1<sup>st</sup> step, dashed: end of second step 19
- Figure 11: Process response to simultaneous step changes in the hydrogen and monomer feed rates towards smaller X 19
- Figure 12: Molecular weight distribution due to simultaneous step changes in the hydrogen and monomer feed rates towards smaller X; dash-and-dot: Normal operating condition, solid: end of first step, dotted: end of second step, dashed: end of third step 20
- Figure 13: Typical step change function 20
- Figure 14: Optimal Hydrogen and Monomer flow rates towards broader MWD with smaller Mw. 23
- Figure 15: MWD for optimal Feed rates towards smaller  $M_w$ ; solid: target function, dotted: optimized, dashed: normal operating condition 23
- Figure 16: Optimal Hydrogen and Monomer flow rates towards broad MWD with high  $M_w$  24
- Figure 17: MWD for optimal Feed rates towards higher  $M_w$ ; solid: target distribution, dotted: optimized, dashed: normal operating condition 24
- Figure 18: Process inputs and outputs when NLMPC is in service 26
- Figure 19: The target and controlled MWD when NLMPC is im service 26

## **ACKNOWLEDGMENT**

The investigators are very grateful to SABIC for supporting this project financially under the program for funding short-term academic research projects. The investigators would also like to thank the general directorate of research center at the college of engineering for their support, continuous follow up and patience throughout the project duration. We would like to emphasize the benefit and advantage of this program, which enables the scientist and scholars to manifest their research ideas into realistic application.

## تطوير خطة تحكم لمدخلات مفاعل البولي الإيثيلين للحصول على مواصفات معينة للبوليمر المنتج

### ملخص

تناقش هذه الدراسة التحديد الأمثل لمدخلات مفاعلات البولي إيثيلين الصناعية بحيث تنتج بلمرات ذات توزيع طول جزيئي محدد. كخطوة أولى تمت نمذجة هذا التوزيع كافتتران معتمد على تركيز الهيدروجين والإيثيلين وكذلك تفاعل البلمرة وسرعته. باستخدام الطرق الرياضية المناسبة، أوجدت أمثل مسارات لتعديل كل من الهيدروجين و الإيثيلين المدخل للمفاعل بحيث نحصل على البوليمر ذي التوزيع الجزيئي المحدد مسبقا. أظهرت الدراسة أهمية كل من نسبة تركيز الهيدروجين إلى تركيز الإيثيلين وكذلك دور سرعة تفاعل البلمرة وسرعة التخلص من الهيدروجين في الحصول على البوليمر المطلوب.

## **ABSTRACT**

This project addresses the issue of determining the optimal input strategies to an industrial polyethylene reactor that produce desired molecular weight distribution of the polymer. The control of entire molecular weight distribution is a complex issue when multisites Ziegler-Natta (Z-N) catalysts are used to produce polyolefins. In this work, the molecular weight distribution is modeled as a function of the reaction kinetics and hydrogen to monomer ratio. Using the control parameterization technique, optimal trajectories for the hydrogen and monomer inlet flow rates were determined such that they produce polyethylene with pre-specified molecular weight distribution. The results showed that, it is necessary to control both polymer properties as well as polymerization reaction rate to get the required distribution. It is also found that optimal input trajectories require at least 15 to 20 hours to affect polymer quality.

## **SUMMARY**

Today, polymers are widely used for various products. Each usage requires different specifications for the polymers. In order to satisfy these demands, companies produce many different grades of polymer. These grades have a different average molecular weight, or (and) a different polydispersity index. However, the residence times of some polymerization reactors, such as loop, tank and fluidized-bed reactors, are normally quite long; therefore, it takes a long time to change over reactor contents. This leads to a greater amount of off-specification polymers produced during grade transition. Since the difference between the market prices of on-specification and off-specification polymers is somewhat large, it is important for a polymer producing company to perform grade transition operations in an optimum way so that minimum amount of off-specification product is produced.

Although the number/weight-average molecular weight and the polydispersity index are widely used as a measure of polymer quality in the polymerization reaction literature, it is very useful to obtain the entire molecular weight distribution to access the shape of the distribution. The control of the entire distribution is an important issue, because in many polymer applications such as paints and paper coatings, it is required to specify such a distribution properly [1, 2]. Furthermore, the molecular weight averages can be misleading when the molecular weight distribution shows bimodalities and/or it has high molecular weight tails. Moreover, although polydispersity is a useful and convenient measure of the width of polymer molecular weight distribution, a polydispersity value itself does not contain enough information about a complete differential molecular weight distribution. It is possible that polymers of different chain length distribution can have the same polydispersity value but exhibit significantly different end-use properties. Thus, there is a strong incentive to develop strategies to control the complete distribution, and not only an average distribution.

In this work, a procedure will be developed to obtain optimal feed profile for the hydrogen flow rate, and possibly other process variables. The optimal strategy will intend to produce polymer with predefined grades. Each grade is defined by the entire molecular

weight distribution instead of the melt index or intrinsic viscosity that is related to polymer average molecular weight. Specifically, the optimal control aims at broadening the molecular weight distribution of the grade. In fact, there is a strong demand to produce polymers having both short and long chains. The presence of short chains is required to give good processability to the polymer; whereas the high molecular weight fraction provides good mechanical properties to the polymer. This makes it desirable to produce polyethylene with a broad molecular weight distribution.

## 1. INTRODUCTION

Polyethylene is considered the world largest produced synthetic commodity polymer. During the past decade, consistency requirements in the polymer properties have led to growing interest in product-quality control schemes for polymerization reactor. Control of polymerization reactors has long been known to be a difficult task, due to high non-linearity of the reactions involved and the strong interaction between the reactor variables. However, there is some reported work on the control of gas phase polymerization of ethylene in fluidized bed reactors. Industrial gas-phase fluidized bed polyethylene reactors are operated in a narrow temperature range between 75 °C and 130 °C and without appropriate temperature control they are known to be prone to unstable behavior, temperature oscillations and incursions toward serious runaway [3], [4].

Stabilization of polyethylene reactors is therefore a challenging problem and needs to be addressed through good control. McAuley and McGregor [5], Dadebo et. al.[6], and Ali et. al.[7], have addressed the stabilization of the reactor temperature through different approaches. Recently Seki et. al. [8] have also studied the stabilization of gas-phase polyethylene reactors through an adequate tuning of PID controller.

The control of grade changeover is another challenging problem in the polyethylene reactor operation. The control objective of the grade changeover is thus to change the polymer properties from one grade to another in the shortest time possible to minimize the off-specs products. In the same time, it is necessary to maintain production rate as constant as possible and to hold reactor pressure within specified bounds to ensure safety. This problem is usually handled as an offline (open-loop mode) optimization problem with free end time. This approach is not only challenging but also requires the absence of modeling error and unmeasured disturbances. This ideal condition; however, does not always exist. There are numbers of efforts in the literature to deal with this issue [9]-[15].

Theoretically, any desired form of the MWD can be produced by appropriate fractionation of very broad molecular weight polymer or blending narrowly distributed

polymers. Fractionation is not employed because of different reasons; the main reason is the extremely high cost of this operation [16]. Blending is not widely used, because most of the catalysts produce widely-distributed polymers. Moreover, producing polymers, which are mixed on a microscale level, requires a melting process. This is not economical.

All the alternative techniques rely on a simple experimental principle: mixing of different polymer materials at the molecular level. This is achieved using one of the following methods:

1. Using a mixture of different metallocenes [17]-[21] or a hybrid catalyst of Ziegler-Natta and metallocene catalysts in a one stage process [22]-[24]. This approach has the advantage that one reactor is required. However, for each polymer grade a sophisticated catalyst has to be developed in order to adjust the amount, the molecular weight distribution, the co-monomer incorporation, and the co-monomer distribution of both fractions formed in the polymerization reaction. Moreover, the mixture of different catalysts may lead to non-reproducible catalyst behavior due to the high variability of the polymerization rate of each catalyst [19]. Additionally, this method depends on implementing a relatively new catalyst that is not widely used industrially. In addition, such implementation requires a deep understanding of polymerization mechanisms using these catalysts; which is not a simple task. Finally, this method is still in the research phase and, it may take a long time before it can be (if it is developed successfully) widely implemented in industry.
2. Polymerization in reactor cascades, where each reactor is operated at different polymerization conditions (usually hydrogen concentration). This technology is already commonly used with Ziegler-Natta catalysts. It has the advantage that only one optimized catalyst is required for the production of various grades. The desired molecular weight distribution and co-monomer distribution are designed by the process. This method is subject to high operational costs [25]. Moreover, it is pointed out that the overall process has a low throughput since two serial processes are employed [26].

3. Variation of polymerization conditions, specially the concentration of chain transfer agents, in a single reactor. This approach has the advantage of requiring a single reactor that simplifies process design and reduces the operational costs. Furthermore, the periodic operation of continuous chemical reactors can improve the performance of the reacting system and allow better design and control of the molecular weight distribution in a single reactor [16], [27]. An example of a process with variation of process conditions is the multizone reactor developed recently by Basell. The problem with the two-step process is that the polymer has low homogeneity of the two (or more) polymer grades and the final polymer particle has a core-shell-like structure. The implementation of a single reactor, compared to implementing two reactors, improves polymer homogeneity and assures that the ratio of both polymer products in each particle is equal to the overall ratio of these products. However, the dynamic operation of the polymerization reactor is difficult and it is subject to appreciable production of off-specification products [25].

Molecular weight distribution broadening that is performed using the second and third approaches implies the production of off-specification products, consequently, the transition period must be as short as possible. Thus, most of the work done in this field focuses on finding the optimal profiles for the manipulated variables.

The objective of this project is to investigate the possibility of obtaining specific polymer quality by special design of the feed flow rates. Specifically, the goal will be to obtain optimal trajectories for the hydrogen, monomer and maybe the catalyst feed flow rates that produce predefined molecular weight distribution.

## **2. THE PROCESS MODEL**

The polyethylene reactor process is depicted in Fig. 1. The process model was developed by [4] and is given below. This model is chosen because its kinetic parameters were validated against plant data [28]. The definition of the various states and parameters of the model is given in the nomenclature.

$$V_g \frac{dC_{M1}}{dt} = F_{M1} - x_{M1}B_t - R_{M1} \quad (1)$$

$$V_g \frac{dC_{M2}}{dt} = F_{M2} - x_{M2}B_t - R_{M2} \quad (2)$$

$$V_g \frac{dC_H}{dt} = F_H - x_H B_t - R_H \quad (3)$$

$$V_g \frac{dC_N}{dt} = F_N - x_N B_t \quad (4)$$

$$\frac{dY_c}{dt} = F_c a_c - k_d Y_c - O_p Y_c / B_w \quad (5)$$

$$(M_r C_{p_r} + B_w C_{p_p}) \frac{dT}{dt} = HF + HG - HR - HT - HP \quad (6)$$

$$M_w C_{p_w} \frac{dT_g}{dt} = F_g C_{p_g} (T_{gi} - T_g) + F_w C_{p_w} (T_{wi} - T_{wo}) \quad (7)$$

$$P_t = (C_{M1} + C_{M2} + C_H + C_N) RT \quad (8)$$

$$T_{gi} = \left( \frac{P_t}{P_t + \Delta P} \right) T \quad (9)$$

$$F_w C_{p_w} (T_{wi} - T_{wo}) = 0.5UA[(T_{wo} + T_{wi}) - (T_{gi} + T_g)] \quad (10)$$

where

$$HF = (F_{M1} C_{p_{M1}} + F_{M2} C_{p_{M2}} + F_H C_{p_H} + F_N C_{p_N}) (T_f - T_{ref}) \quad (11)$$

$$HG = F_g C_{p_g} (T_g - T_{ref}) \quad (12)$$

$$HT = (F_g + B_t) C_{p_g} (T - T_{ref}) \quad (13)$$

$$HP = O_p C_{p_p} (T - T_{ref}) \quad (14)$$

$$HR = M_{w1} R_{M1} \Delta H_r \quad (15)$$

$$O_p = M_{w1} R_{M1} + M_{w2} R_{M2} \quad (16)$$

$$R_{M1} = C_{M1} Y_c k_{p1} e^{-\frac{E}{R}(1/T - 1/T_{ref})} \quad (17)$$

$$R_{M2} = C_{M2} Y_c k_{p2} e^{\frac{-E}{R}(1/T-1/T_{ref})} \quad (18)$$

$$Cp_g = \sum x_i Cp_i \quad (19)$$

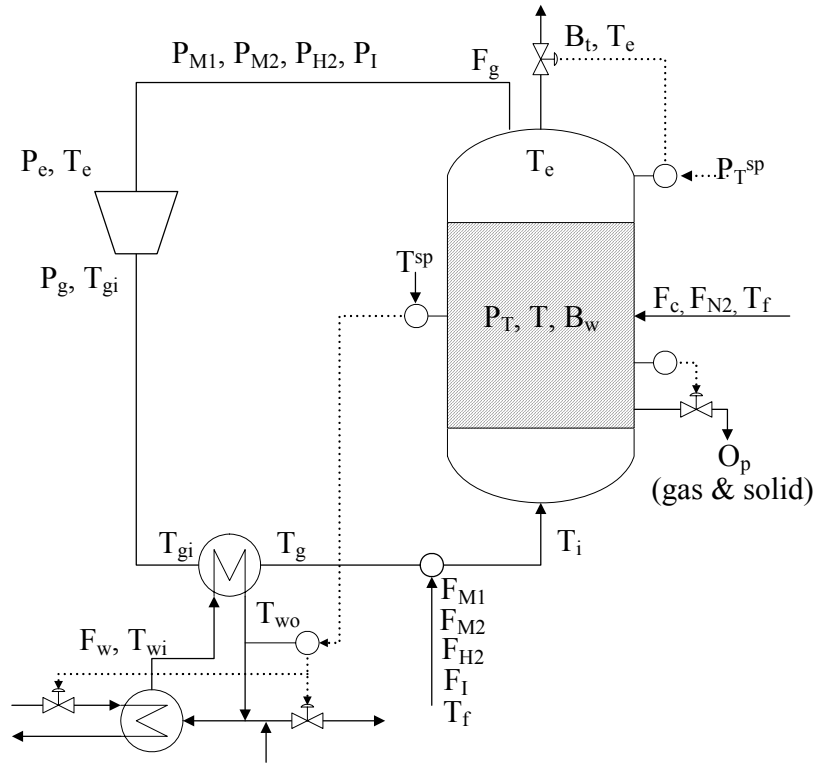


Fig. 1: schematic of the polyethylene reactor

The model equations listed above are slightly modified than those given by [4]. For simplicity, the energy balance around the cooler considers the dynamic of the recycle temperature explicitly instead of the heat removal as used by [4]. In due course, the cooling process is modeled as well mixed system. The thermal effect of the recycle compressor is also included in this model. Note that the partial pressure of the reactants can be calculated directly from the reactant concentrations using ideal gas law.

## 2.1 PLANT OPERATING CONDITION

In addition to the above modification, the utilization of the model is more comprehensive in this work. Although, McAuley et al. [4] have determined all the process parameters, they have not determined the steady state operation condition for the entire process variables. The steady state values for  $C_{M2}$ ,  $C_H$ ,  $C_N$ ,  $Y_c$ ,  $T_{wo}$ ,  $T_g$ ,  $F_{M2}$ ,  $F_N$  and  $F_H$  were not determined. This is because the authors focused their analysis only on the reactor temperature and the monomer concentration. In this work, the objective is to control the partial pressures of the gases, the total pressure and the reactor temperature. Therefore, an initial steady state for the entire process should be determined. One operating condition can be determined from solving the following steady state optimization problem:

$$\min_{C_{M1}, C_{M2}, C_H, C_N, Y_c, T, F_{M2}, F_H, F_N, B_t, UA, T_{wo}, T_g} \phi = \left\| P_{M1} - P_{M1}^* \right\|^2 + \left\| P_t - P_t^* \right\|^2 \quad (20)$$

subject to:

$$h = f(\bar{X}, \bar{U}) = 0 \quad (21)$$

The process operating conditions, i.e. the values of the parameters shown in the objective function, are determined such that the monomer partial pressure and the total pressure are fixed at the desired industrial values ( $P_{M1}^*$ ,  $P_t^*$ ), while satisfying the algebraic constraints,  $h$  that represent the steady state model. The desired values for  $P_{MI}$  fall in the range [7~9 atm] while that for the total pressure falls in the range of [18~24 atm]. The algebraic constraints contain  $\bar{X}$ , which denotes the vector of all process states, and  $\bar{U}$ , which denotes the vector of all process inputs. The remaining variables and parameters that are not included in the set of design parameters in the above minimization problem are fixed at their nominal values as given by [4]. The results of the optimization problem are listed in Table 1 while the values of the other fixed parameters are given in Table 2. To be able to make use of the dynamic model, the value of the holdup inside the cooler,  $M_w$ , needs to be determined. The value is assumed to be around  $2 \times 10^6$  moles, which is estimated roughly from the cooler residence time given by [4] and from the coolant flow rate.

**Table 1: steady state operating condition**

$C_{MI}$	297.06 mole/m <sup>3</sup>	$F_{MI}$	131.13 mole/s	$Y_c$	5.849 mole	$T_g$	324.7 K
$C_{M2}$	116.17 mole/m <sup>3</sup>	$F_{M2}$	3.5100 mole/s	$T$	82.7 °C	$T_{wo}$	308 K
$C_H$	105.78 mole/m <sup>3</sup>	$F_H$	1.6000 mole/s	$B_t$	10.39 mole/s	$T_{wi}$	293 K
$C_N$	166.23 mole/m <sup>3</sup>	$F_N$	2.5200 mole/s	$F_w$	3.11x10 <sup>4</sup> mole/s	$F_c$	2 kg/hr

**Table 2: process parameters**

$B_w$	70x10 <sup>7</sup> g	$\Delta H_r$	-894 cal/g	$k_{p1}$	85 L/mole.s	$C_{pH}$	7.7 cal/mole.K
$C_{pp}$	0.85 cal/g.K	$k_d$	0 1/s	$k_{p2}$	3 L/mole.s	$C_{pMI}$	11 cal/mole.K
$E$	9000 cal/mole	$M_r C_{pr}$	1400 kcal/K	$T_f$	293 K	$C_{pN}$	6.9 cal/mole.K
$V_g$	500 m <sup>3</sup>	$F_g$	8500 mole/s	$\Delta P$	3 atm	$C_{pM2}$	24 cal/mole.K
$T_{ref}$	360 K	$UA$	1.263x10 <sup>5</sup> cal/s.K	$a_c$	0.548 mole/kg	$C_{pw}$	18 cal/mole.K

## 2.2 THE POLYMER PROPERTIES MODEL

It is well known that a number of mechanical properties of the polymer such as stiffness, Transparency, hardness as well as rheological and processability characteristics are strongly related to the Melt Index (MI) and density. Melt Index and density of the formed polymer can be related to the gases molar ratio according to [4] as follows:

$$\ln(MI) = 3.5 \ln \left( k_0 + k_1 \frac{[M_2]}{[M_1]} + k_3 \frac{[H_2]}{[M_1]} \right) \quad (22)$$

$$\rho = p_0 + p_1 \ln(MI) - \left( p_2 \frac{[M_2]}{[M_1]} + p_3 \frac{[M_3]}{[M_1]} \right)^{p_4} \quad (23)$$

Where

$$k_0=0.4; k_1=1.5; k_3=2.2$$

$$p_0=0.96; p_1=0.0025; p_2=0.007; p_4=0.5$$

The cumulative Melt index and polymer density can be obtained from the following ODE:

$$\frac{dMI_c}{dt} = \frac{3.5O_p}{B_w} \left( MI_c^{\frac{1}{3.5}} MI_c^{\frac{2.5}{3.5}} - MI_c \right) \quad (24)$$

$$\frac{d(1/\rho_c)}{dt} = \frac{O_p}{B_w} \left( \frac{1}{\rho} - \frac{1}{\rho_c} \right) \quad (25)$$

The instantaneous molecular weight distribution for each type of active sites is given by the following equation:

$$y_j^d = j \cdot q^2 \cdot \exp(-j \cdot q) \quad (26)$$

While the cumulative distribution is given by:

$$\frac{dy_j}{dt} = \frac{O_p \cdot (y_j^d - y_j)}{B_w} \quad (27)$$

Finally the gel permeation chromatography (GPC) reading of the molecular weight distribution (MWD) is calculated by the following:

$$GPC = j \cdot y_j^d \cdot \ln(10) \quad (28)$$

In the above equations,  $j$  is the number of repeating units and  $q$  is the chain termination probability, it is defined as  $q = [\text{sum of chain-termination rates}]/[\text{chain propagation rate}]$  and can be computed from:

$$q = \frac{k_{tm} + k_{th}X}{k_m + k_{th}X + k_p} \quad (29)$$

In the last equation,  $X$  denotes the molar ratio of hydrogen to monomer inside the reactor. This ratio is a crucial parameter to vary the value of  $q$  and consequently the molecular weight distribution. Careful adjustment of  $q$  is necessary to achieve desired polymer properties as it will be discussed in the results section.

### 3. THE ON-LINE NLMPC ALGORITHM

In this work, the structure of the model predictive control (MPC) version developed by [29] that utilizes directly the nonlinear model for output prediction is used. A usual MPC formulation solves the following on-line optimization:

$$\min_{\Delta u(t_k), \dots, \Delta u(t_{k+M-1})} \sum_{i=1}^P \|\Gamma(y(t_{k+i}) - R(t_{k+i}))\|^2 + \sum_{i=1}^M \|\Lambda \Delta u(t_{k+i-1})\|^2 \quad (30)$$

subject to

$$A^T \Delta U(t_k) \leq b \quad (31)$$

For nonlinear MPC, the predicted output,  $y$  over the prediction horizon  $P$  is obtained by the numerical integration of:

$$\frac{dx}{dt} = f(x, u, t) \quad (32)$$

$$y = g(x) \quad (33)$$

from  $t_k$  up to  $t_{k+P}$  where  $x$  and  $y$  represent the states and the output of the model, respectively. The symbols  $\|\cdot\|$  denotes the Euclidean norm,  $k$  is the sampling instant,  $\Gamma$  and  $\Lambda$  are diagonal weight matrices and  $R = [r(k+1) \dots r(k+P)]^T$  is a vector of the desired output trajectory.  $\Delta U(t_k) = [\Delta u(t_k) \dots \Delta u(t_{k+M-1})]^T$  is a vector of  $M$  future changes of the manipulated variable vector  $u$  that are to be determined by the on-line optimization. The control horizon ( $M$ ) and the prediction horizon ( $P$ ) are used to adjust the speed of the response and hence to stabilize the feedback behavior.  $\Gamma$  is usually used for trade-off between different controlled outputs. The input move suppression,  $\Lambda$ , on the other hand, is used to penalize different inputs and thus to stabilize the feedback response. The objective function (30) is solved on-line to determine the optimum value of  $\Delta U(t_k)$ . Only the current

value of  $\Delta u$ , which is the first element of  $\Delta U(t_k)$ , is implemented on the plant. At the next sampling instant, the whole procedure is repeated.

To compensate for modeling error and eliminate steady state offset, a regular feedback is incorporated on the output predictions,  $y(t_{k+1})$  through an additive disturbance term. Therefore, the output prediction is corrected by adding to it the disturbance estimates. The latter is set equal to the difference between plant and model outputs at present time  $k$  as follows:

$$d(k) = y_p(k) - y(k) \quad (34)$$

The disturbance estimate,  $d$  is assumed constant over the prediction horizon due to the lack of an explicit means of predicting the disturbance. However, for severe modeling errors, or open-loop unstable processes the regular feedback is not enough to improve the NLMCP response. Hence, state or parameter estimation is necessary to enhance the NLMPC performance in the face of model-plant mismatch. In this work, Kalman filtering (KF) will be incorporated to correct the model state and thus, to address the robustness issue. Utilization of the NLMPC with KF requires adjusting an additional parameter,  $\sigma$ . More details on the integration of KF with the NLMCP algorithm are given elsewhere [29]. In addition to state estimation by KF, the predicted output will be also corrected by the additive disturbance estimates of (34).

#### 4. RESULTS

First we simulate the model for the operating condition shown in Table 1 and 2. Figs. 2-4 show the dynamic response of the plant various variables at fixed value for the process inputs. For this specific operating condition, the molar ratio of hydrogen to monomer inside the reactor is around 0.35. Fig. 4 shows a relatively narrow molecular weight distribution with polydispersity index of 3.0 and weight average molecular weight of 42 kg/mole. The next objective is to show how manipulating the feed flow rates, a different molecular weight distribution can be obtained.

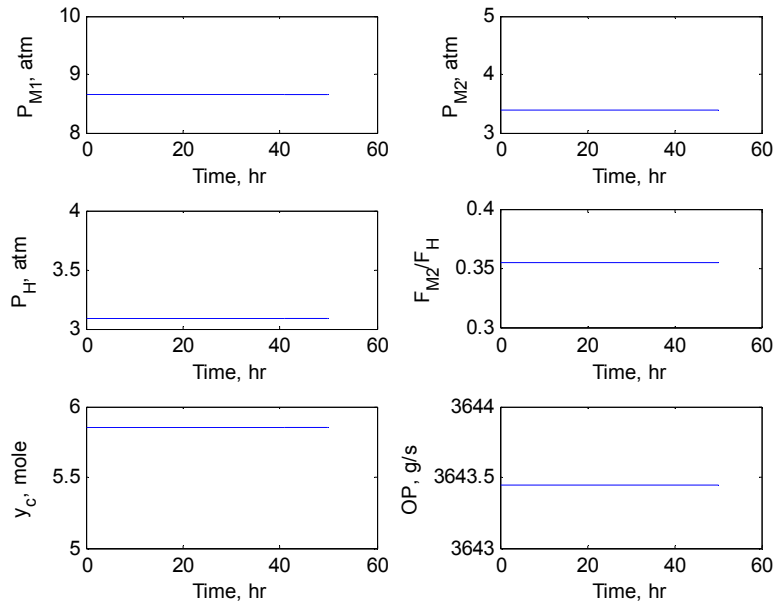


Fig. 2: Process outputs at the normal operating condition

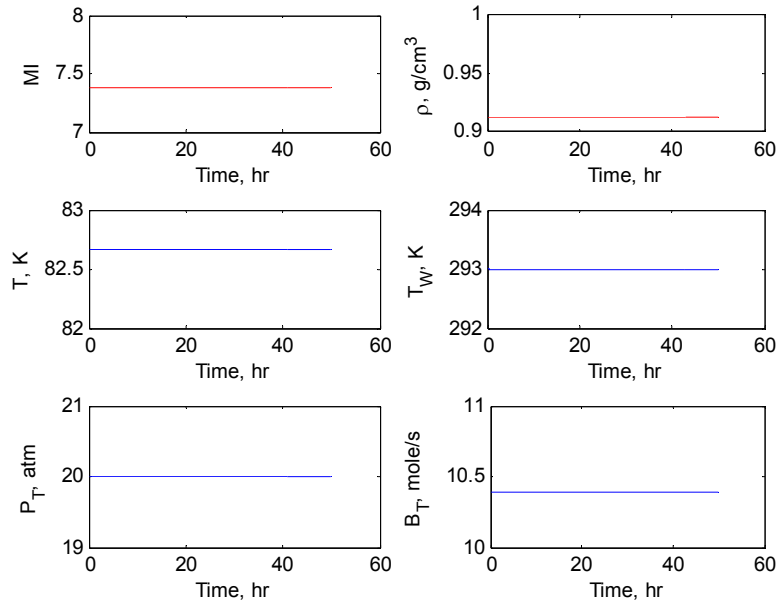


Fig. 3: The polymer properties and the controlled process variables at the normal operating condition

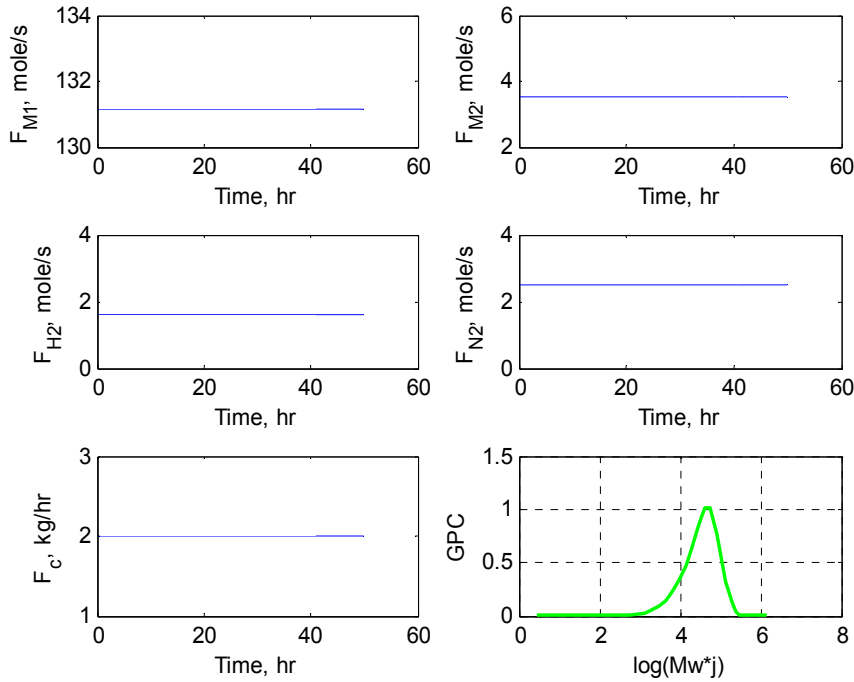


Fig. 4: Process inputs and the molecular weight distribution at the normal operating condition

#### 4.1 EFFECT OF HYDROGEN FEED FLOW RATE

It is believed that altering the hydrogen concentration inside the reactor affects polymerization reaction kinetics and therefore the polymer quality. For this purpose, we will study the impact of changing the hydrogen feed flow rate while keeping the monomer feed rate constant. Fig. 5 and 6 simulate the process for a positive step change in hydrogen feed rate to a maximum value for about 9 hours followed by a negative step change to zero value. The idea of this aggressive step changes is to create sharp and sudden changes in the hydrogen content inside the reactor and consequently in the molar ratio of the hydrogen to monomer. Long duration for each step change is employed to provide enough time for the hydrogen pressure to respond. As it can be seen from Fig. 5, these considerable changes in hydrogen feed rate made a little effect in the hydrogen pressure and its ratio to monomer pressure. For this reason the molecular weight distribution, in terms of broadening and average molecular weight distribution, is barely affected as shown in Fig. 6. The marginal variation in hydrogen pressure is contributed to its slow dynamics bearing in mind that

hydrogen is not consumed by the reaction. It is worth mentioning that hydrogen usually decreases ethylene polymerization rate. However, this effect depends on Ziegler-Natta catalyst generation and hydrogen concentration inside the reactor as well. In this work, hydrogen effect is very small, Fig. 5, so that it can be ignored. This means that hydrogen can be used only to control the molecular weight distribution of the produced polymer; whereas, other variables, such as monomer feed rate and polymerization temperature, can be used to control the polymerization rate.

Fig. 7 and 8 illustrate the system reaction to variations in the hydrogen feed flow rate but in the opposite direction. Specifically, the hydrogen feed rate is brought to its minimum value for the first 9 hours and then increased to its upper value. Once again, the slow dynamic of the hydrogen pressure inside the reactor hindered the  $H_2/M_1$  ratio from changing considerably. As a result the molecular weight distribution is not affected as shown in Fig. 8. Many other attempts with different amplitude and duration for the step changes were tried. However, no significant results were obtained because the hydrogen transient response is very slow. Our investigation indicated that broader MWD can be obtained but at step changes with very large duration periods that exceed the reactor residence time by many folds which is impractical.

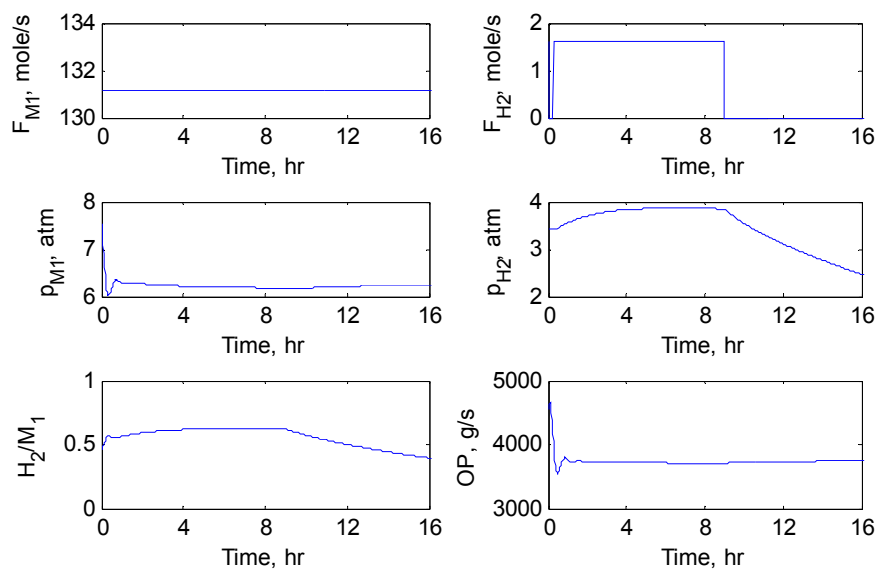


Fig. 5: Process Responses for Hydrogen up-down Step changes

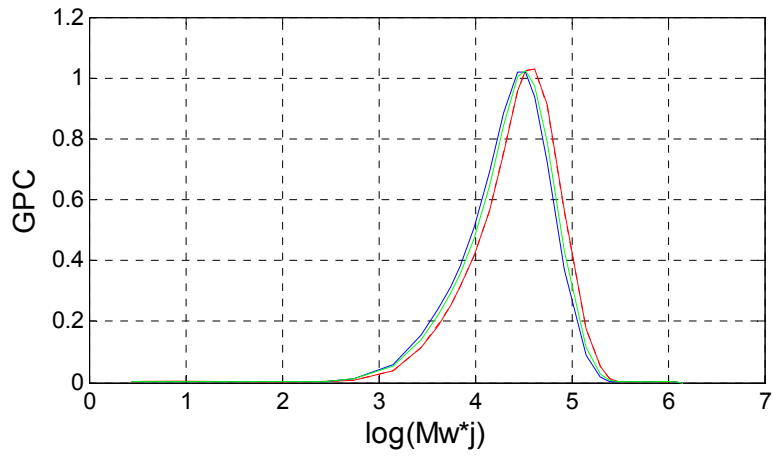


Fig. 6: Molecular weight distribution for hydrogen up-down step changes

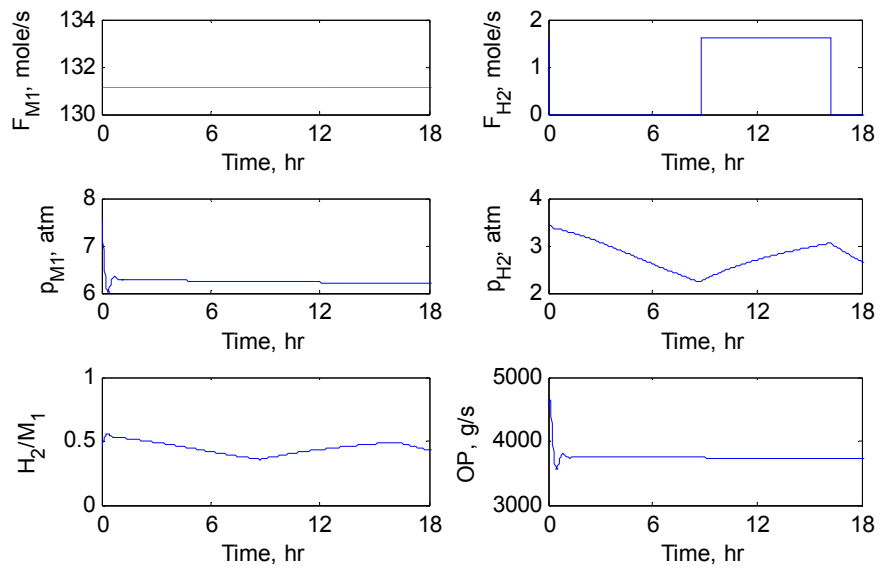


Fig. 7: Process Response to down-up changes in the hydrogen fed flow rate

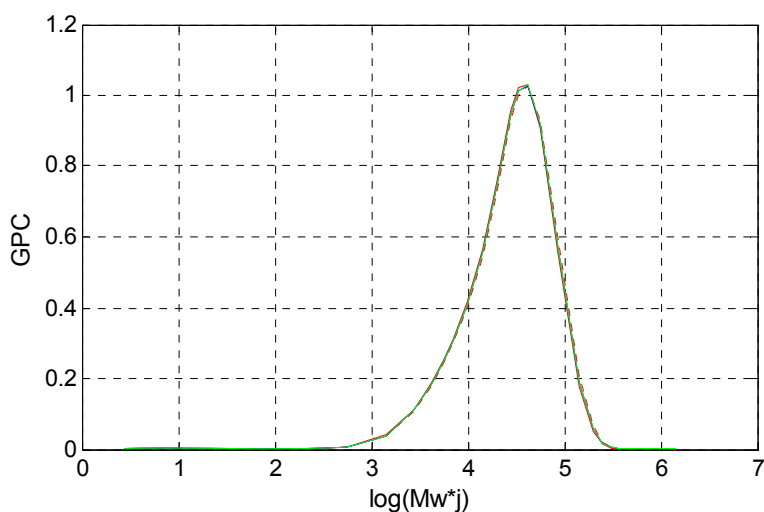


Fig. 8: Molecular weight distribution due to down-up changes in the hydrogen feed flow rate

#### 4.2 EFFECT OF MONOMER AND HYDROGEN FEED FLOW RATES

The previous tests revealed that the slow dynamics of the hydrogen pressure inside the reactor prevents getting quick alteration of the hydrogen to monomer ratio ( $X$ ). To speed up the  $X$  response, the monomer feed flow will be changed in coordination with the hydrogen feed flow rate. Figs. 9 and 10 depicted the result when both the hydrogen and monomer flow rates are varied between their extreme values. It is obvious that changing the hydrogen and monomer flow rates simultaneously helped in increasing  $X$  rapidly. Increasing the ratio to a high value and suddenly decreasing it managed to alter the distribution of the polymer molecular weight as shown in Fig. 10. The solid curve in Fig. 10 corresponds to the initial operating condition, i.e. before increasing  $X$ . The dotted curve corresponds to the beginning of the second switching point (Maximum ratio) which occurs around 9 hours while the dashed curve denotes the MWD at the end of the second switching point, i.e. around 16.5 hours. The dotted curve proves that this strategy largely broadens the distribution so that bimodal distribution can be obtained by manipulating the feed flow rates. However, this is achieved at the expense of high molar ratio,  $X \sim 5.0$ .

Alternatively, we tried to investigate the effect of operating at smaller  $X$ . Fig. 10 and 11 simulate the process response to such direction. It can be seen that setting the monomer feed rate at maximum and the hydrogen feed rate at minimum for the first 17 hours

followed by flipping the low rates will impact the MWD considerably. Clearly, Fig. 11 shows that the MWD becomes broader. Moreover, the distribution moves towards polymer with higher average molecular weight. It should be noted though, that somehow long period is used. It took 20 hours of operation to obtain the broadened MWD. Slightly shorter periods can still produce wider MWD, but no less than 15 hours.

In all previous tests, the amplitude of the step changes was set to their extreme values and the duration of the step changes were adjusted manually. In the next tests, we will try to optimize the cycle period, i.e. the duration of each step change.

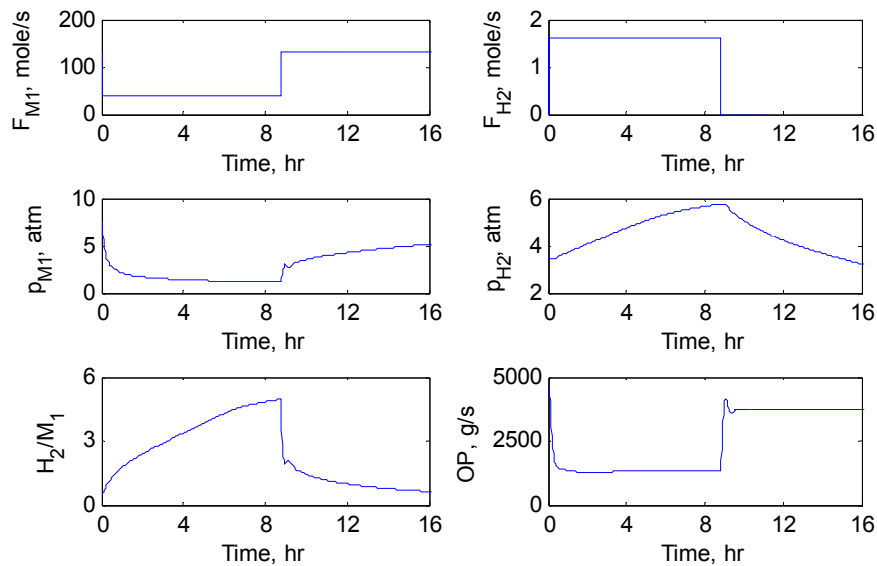


Fig. 9: Process response to simultaneous changes in the hydrogen and monomer flow rates towards higher X.

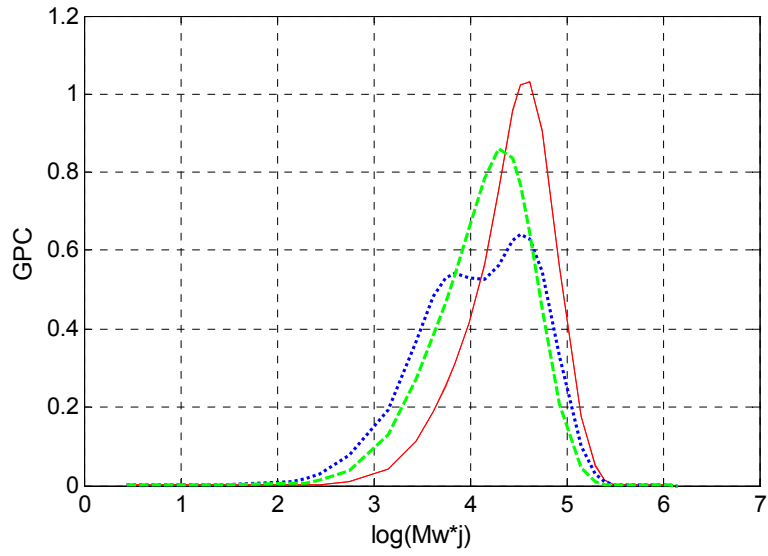


Fig. 10: Molecular weight distribution due to simultaneous changes in the hydrogen and monomer flow rates towards higher X; solid: start of 1<sup>st</sup> step (normal operating condition), dotted: end of 1<sup>st</sup> step, dashed: end of second step

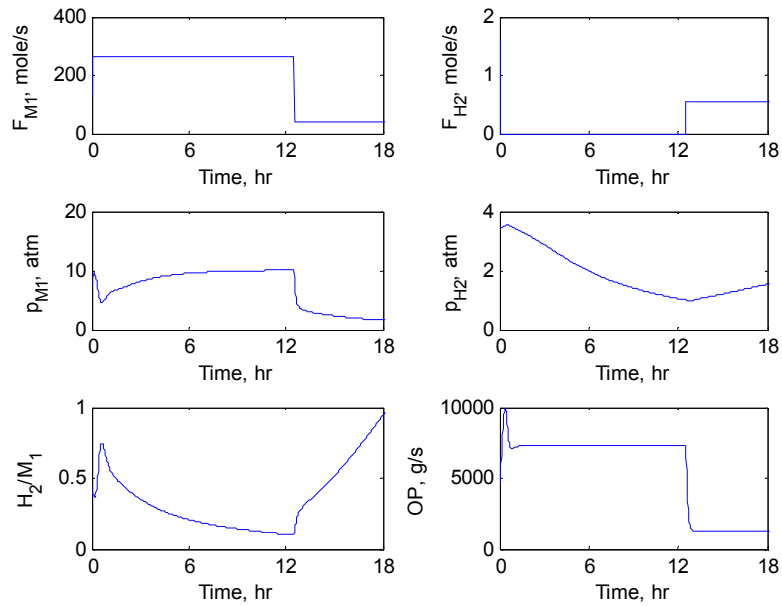
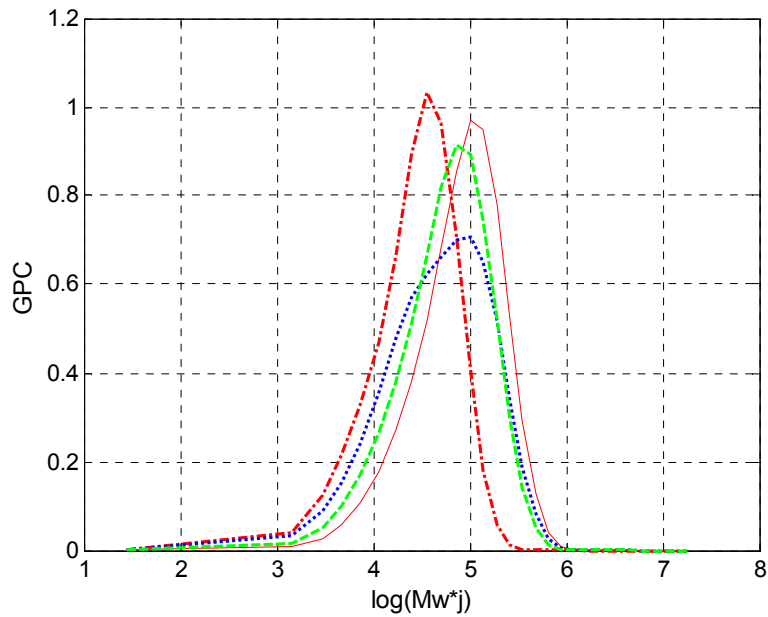


Fig. 11: Process response to simultaneous step changes in the hydrogen and monomer feed rates towards smaller X



**Fig. 12:** Molecular weight distribution due to simultaneous step changes in the hydrogen and monomer feed rates towards smaller X; dash-and-dot: Normal operating condition, solid: end of first step, dotted: end of second step, dashed: end of third step

### 4.3 OPTIMAL STEP CHANGES

The step changes parameters in all previous tests were chosen arbitrary. Extreme values were used for the amplitude for the sake of achieving fast dynamic response. These values caused excessive changes in the production rate and reactor temperature. Therefore, the amplitude of the step changes can be optimized to avoid such a situation. Furthermore, it is favorable to move to another MWD in a short time. Therefore, the step change duration can also be optimized for this purpose.

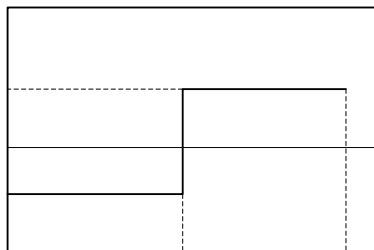


**Fig. 13:** Typical step change function

The inlet flow rates are injected into the process as a square wave, i.e. a series of up and down step changes as shown in Fig. 13. This input wave consists of four parameters that need to be designed. The step duration  $d_1$  and  $d_2$  and the step amplitude  $a_1$  and  $a_2$ . The nominal value for a specific inlet flow rate is  $u_0$ . One way to optimally select the value of these parameters is to solve this cost function:

$$\min_{d_1, d_2, z} \int_{t_0}^{t_f} \sum_{i=1}^N (GPC_i(t) - GPC_i^T)^2 dt \quad (35)$$

Where  $GPC^T$  is the target MWD,  $N$  is the number of GPC elements, usually five points, i.e.  $N=5$ , gauntless accurate description of the MWD.  $t_0$  is the time at which the grade transition begins and  $t_f$  is the control horizon. This parameter can be chosen either well beyond the end of the transition period when the reactor reaches steady state, or it can be treated as a decision variable and augmented in the optimization problem. The amplitude of the square wave is related to  $z$  as follows:

$$a_1 = z * u_0; \quad a_2 = (z^u - z) * u_0 \quad (36)$$

Note that the design parameters mentioned above are for single flow rate. For two inlet flow rates (Hydrogen and Monomer) the design parameters become 6 while the cost function remains the same. The optimization problem is solved numerically based on the following bounds:

$$\begin{aligned} 0.5 &\leq d_1 \leq 10 \\ 0.5 &\leq d_2 \leq 10 \\ z^l &\leq z \leq z^u \end{aligned}$$

In the above equations  $z$  is a fraction of the nominal value for the process input. The lower and upper value of  $z$  will vary with type of inlet flow and target type (i.e. high or low  $X$ ) as will be discussed later. First we test the case of shifting the MWD to the left, i.e. towards smaller  $M_w$ . In due course, we are seeking larger  $X$ . Therefore, the lower and upper limits for  $z$  for the hydrogen flow rate is (0,1) and that for monomer flow rate is (0.2,1). Here zero value for the monomer lower limit is avoided to avoid excessive increase of the  $X$ . The

target GPC in (35) is taken from the step change responses. For example, if lower  $X$  is sought, then the dotted curve in Fig. 10 is taken as the target MWD. On the other hand, if higher  $X$  is sought, here the dotted curve in Fig. 12 is considered as the target function.

The results of the optimization problem considering the lower  $X$  target are shown in Figs. 14 and 15. The optimization is carried over a simulation time of 25 hours. The method managed to create a long periods of high hydrogen flow and low monomer flow, a situation that results in a high  $X$ . The latter produced broad bimodal MWD. As expected, the resulted average  $M_w$  is less than that at the nominal conditions. Note that the target function is designed such that it flattens the shape of the GPC and move it towards the left. The solution of the optimization problem created different input sequence than that shown in Fig. 9. It is obvious that this situation decreases considerable polymer production rate because of the minimal monomer feed flow rate. It is worth mentioning that to compensate for the decrease in monomer concentration, catalyst federate can be optimized to keep polymer production rate near its target value. However, such scenario is beyond the objectives of this work.

The Optimization problem is also solved for the case of producing higher  $M_w$ . The results are shown in Figs. 16 and 17. The lower and upper limits for  $z$  for the hydrogen flow rate is (0,0.4) and that for monomer flow rate is (0.6,2). The small value or the upper limit for hydrogen and large value for the lower limit for monomer is employed to avoid large  $X$  and the large value for the upper limit fir monomer is chosen such that it provides minimal  $X$ . The target function is designed such that it flattens the MWD and moves towards higher  $M_w$ . Obviously, the procedure helped in developing input sequences that created the broad MWD shown in Fig. 17.

Despite the success of the above methods, the input sequences created fluctuation in the reactor temperature (not shown here), and production rate. The temperature fluctuation is taken care of by the temperature control loop. However, better control design is needed because the input sequences may become aggressive. On the other hand, the fluctuation in

the production rate and the polymer properties should be take care of by incorporating them in the cost function.

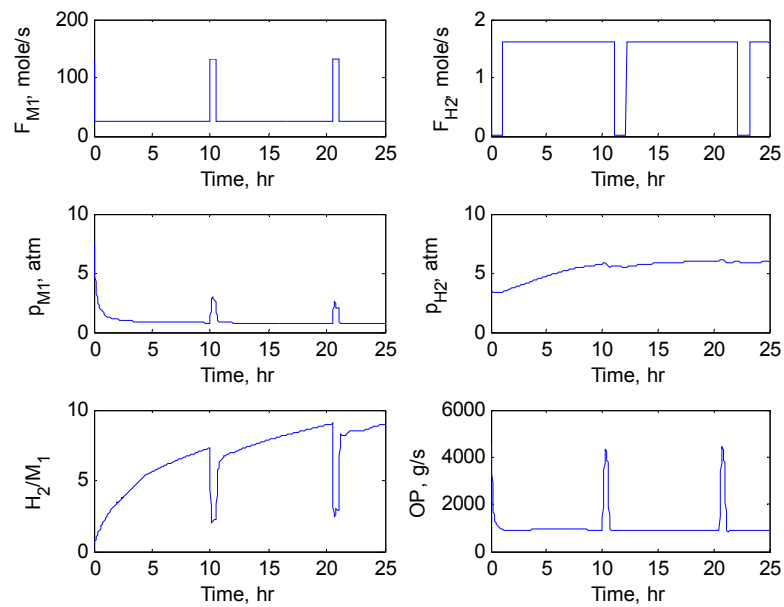


**Fig. 14:** Optimal Hydrogen and Monomer flow rates towards broader MWD with smaller  $M_w$ .

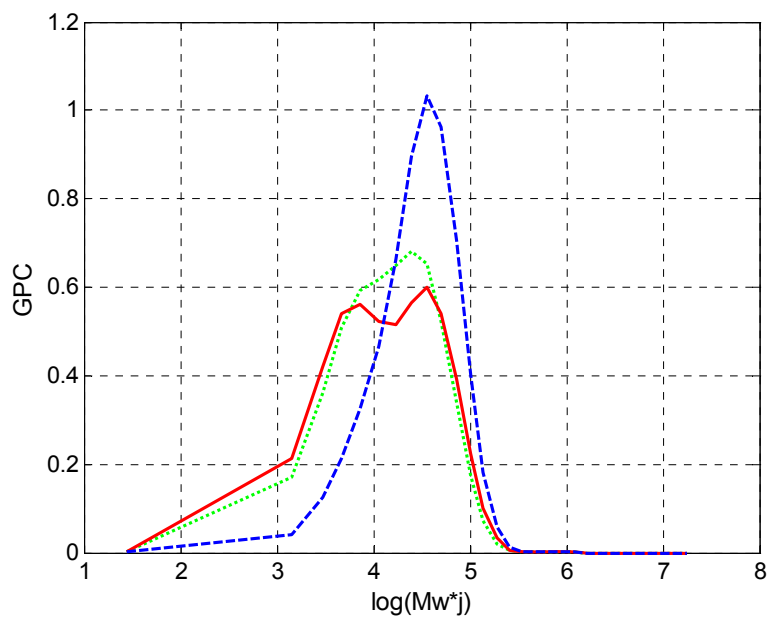


**Fig. 15:** MWD for optimal Feed rates towards smaller  $M_w$ ; solid: target function, dotted: optimized, dashed: normal operating condition

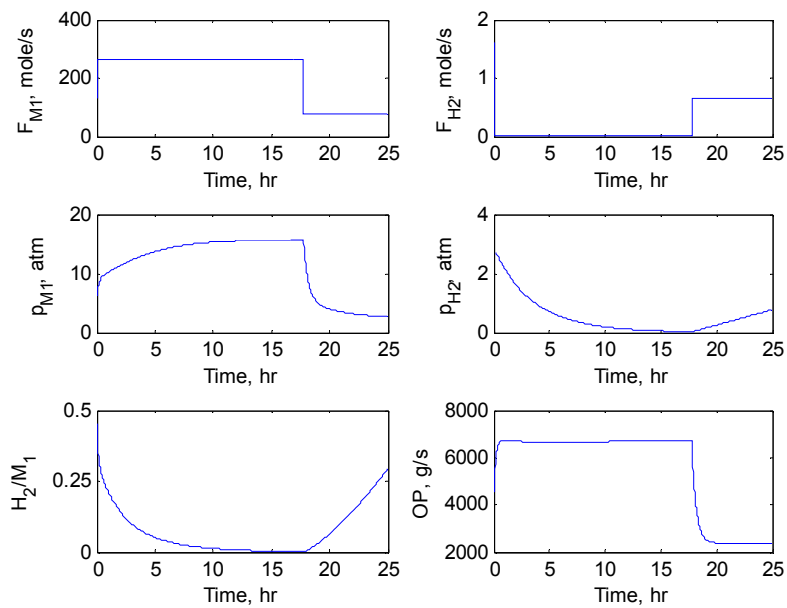


Fig. 16: Optimal Hydrogen and Monomer flow rates towards broad MWD with high  $M_w$

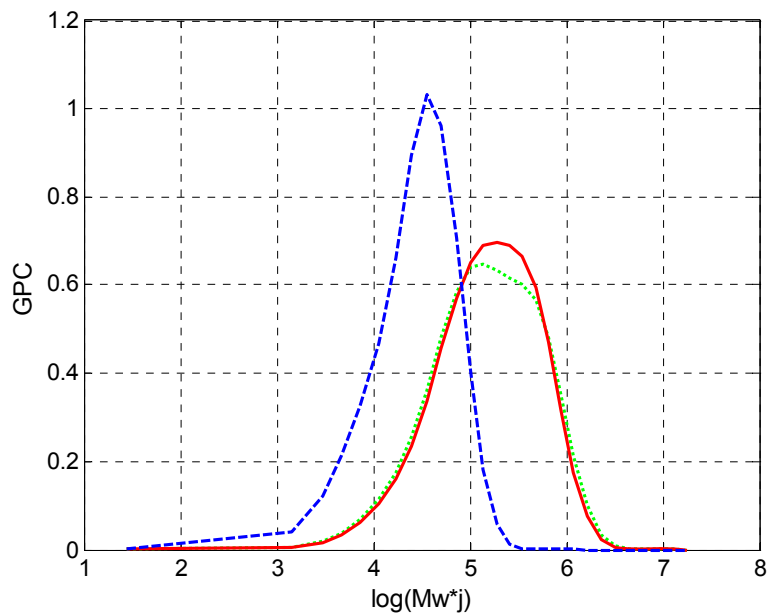
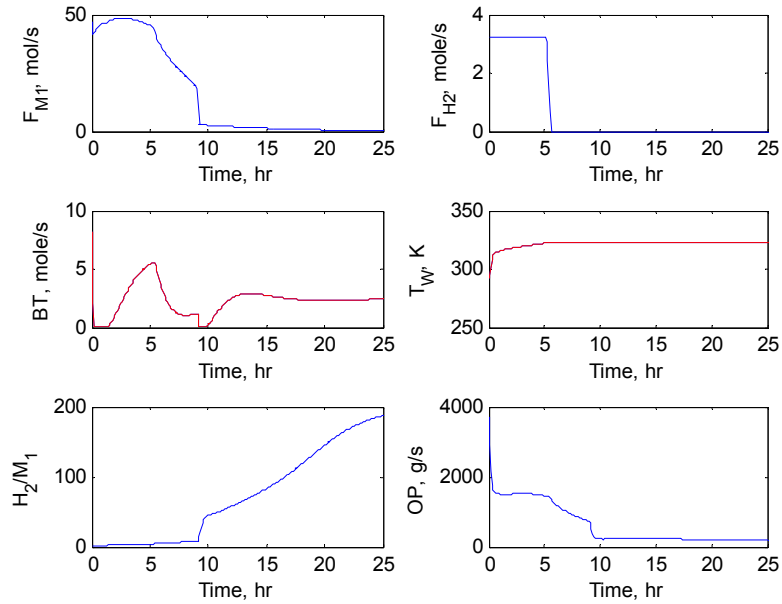


Fig. 17: MWD for optimal Feed rates towards higher  $M_w$ ; solid: target distribution, dotted: optimized, dashed: normal operating condition

#### 4.4 Online Optimization

As mentioned in the previous section, obtaining input trajectories that provide desired MWD is difficult as the final polymer quality is very sensitive to the value of  $X$  and to the dynamics of the polymerization rate. In this sense, maintaining the desired MWD during process operation is even more challenging. In the presence of model-plant mismatch and/or when unmeasured disturbances enter the plant, the situation becomes more complex. For this purpose, we will test the effectiveness of nonlinear Model Predictive Control to handle this issue. The control objective here is to move the operating point from the normal one to the one shown in Fig. 15 and maintain it at that value. The result of this case is shown in Fig. 18 and 19. Two manipulated variables, which are the monomer and hydrogen flow rates, are used. The weighting factor for these inputs is  $\Lambda=[1 \ 1]$ . Eight controlled variables, which represent specific points in the target MWD, are considered as shown by the red dots in Fig. 19. The weighting factor for all outputs is given the same value of  $\gamma=100$ . The MWD target function contains 28 points, however only eight points were selected as controlled outputs to reduce the computation effort consumed by the NLMPC calculations. The input (M) and output (P) horizons are taken equal to 1 and 40, respectively. Fig. 18, illustrates how the manipulated variables  $F_{M1}$  and  $F_{H2}$  are altered by NLMPC in order to obtain the MWD shown in Fig. 19. Moreover, Fig. 18 shows how the bled flow rate and the cooling water inlet temperature varies by a separate PI controllers to maintain the total pressure at 20 atm and the reactor temperature at 82 °C. Fig. 19 depicts the target and controlled MWD. Obviously, NLMPC managed to bring the process MWD within the target but at high  $X$  and very low production rate as shown in Fig. 18. Once again, this is the same observation discussed earlier in section 4.2. This preliminary result is promising but further work is needed to investigate the possibility to keep  $X$  and OP within acceptable values and to test the effectiveness of NLMPC to reject the effect of model uncertainty and/or unmeasured disturbances. Additional work is also needed to examine the capability of NLMPC to operate the process around the operating condition of higher average molecular weight in the absence and in the presence of modeling errors and/or unmeasured disturbances.



**Fig. 18: Process inputs and outputs when NLMPC is in service**

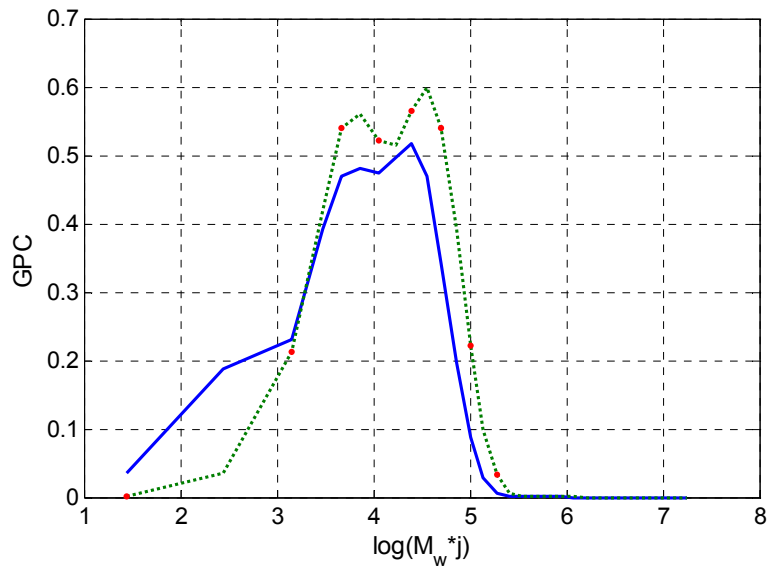


**Fig. 19: The target and controlled MWD when NLMPC is in service**

## 5. CONCLUSIONS

Producing polymers with specific rheological and mechanical properties is an important aspect of the polyethylene industry. These properties are controlled by the microstructure of the produced polymer. Among different polymer properties, polymer processability is considered as one of the major properties of the polymer that determines its final application. Processability is highly affected by the molecular weight distribution of the polymer. This distribution can be controlled in different ways. One of the most effective approaches is to change the operating conditions inside the reactor during the polymerization reaction. Using this approach, the major role is played by hydrogen to the monomer ratio that affects not only molecular weight distribution of the polymer but also the polymerization kinetics itself. Other important variables are catalyst concentration and polymerization temperature. The MWD is modeled as a function of the reaction kinetics and hydrogen to monomer ratio and its effect on the MWD is investigated. It is found that manipulating hydrogen flow rate solely can affect the MWD within certain time limit because of its very slow dynamics. Whereas, simultaneous alteration of the hydrogen and monomer flow rates within a period of 20 hours can create significant effect on the MWD. In fact, optimal input sequences for the hydrogen and monomer inlet flow that produces broad MWD was obtained. Further investigation is required to reduce the sequence duration in order to minimize the off specs products. It is also found that possibilities for broadening the molecular weight distribution depend strongly on the ability to remove hydrogen from the reactor. For example, the use of catalyst systems which are highly sensitive to hydrogen, such as Ziegler-Natta catalyst with diether as an internal donor, might give better results than use of the existing catalyst. This is due to the fact that diether-catalyst is more sensitive to hydrogen, so that small amounts of hydrogen are required for polymer molecular weight control. Further study is required to implement the optimal broadening strategy on-line, which is challenging due to the long times required to calculate the optimal trajectories. Alternating the type of the fed catalyst to the reactor during operation is also another challenging issue.

## 6. NOMENCLATURE

$A$	Constant matrix for linear constraints
$a_c$	Active site concentration, mole/kg
$b$	Vector of upper and lower bounds for the linear constraints
$B_w$	Mass of the polymer in the bed, gm
$B_t$	Bleed flow rate, mole/s
$C_{M1}, C_{M2}, C_N, C_H$	Concentration monomer, co-monomer, nitrogen, and hydrogen, mole/m <sup>3</sup>
$C_{PM1}, C_{PM2}, C_{PH}, C_{PN}$	Heat capacity of monomer, co-monomer, hydrogen and nitrogen, cal/mole K
$C_{pg}, C_{pw}$	Heat capacity of recycle gas and water cal/mole K
$C_{pp}$	Heat capacity of polymer, cal/g K
$E$	Activation energy for propagation, cal/mole
$F_c$	Catalyst flow rate. kg/s
$F_w, F_g$	Cooling water and recycle flow rate, mole/s
$F_{M1}, F_{M2}, F_H, F_N$	Monomer, co-monomer, hydrogen and nitrogen flow rate, mole/s
$HF, HG, HP$	Sensible heat of fresh feed, recycle gas and product, cal/s
$HR$	Enthalpy generated from ethylene polymerization, cal/s
$k_d$	Deactivation rate constant, 1/s
$k_{p1}, k_{p2}$	Propagation rate constant for monomer and co-monomer, L/mole s
$k_{th}$	Reaction rate constant for chain transfer to hydrogen, m <sup>3</sup> /mol s
$Kp$	Propagation reaction rate constant, m <sup>3</sup> /mole s
$k_{tm}$	Reaction rate constant for chain transfer to monomer, m <sup>3</sup> /mol s
$M, M_p$	Control horizon, constant matrix
$M_w$	Water holdup in the heat exchanger, mole
$M_r, C_{pr}$	Thermal capacitance of the reaction vessel, kcal/K
$Op$	Polymer outlet rate, kg/s
$P$	Prediction horizon
$P_t$	Total pressure, atmosphere
$P_{M1}, P_{M2}, P_N, P_H$	Partial pressure of monomer, co-monomer, nitrogen and hydrogen, atm

$q$	chain termination probability
$R$	Ideal Gas constant, atm m <sup>3</sup> /K mole also vector of set points
$R_{M1}, R_{M2}, R_H$	Consumption rate of monomer, co-monomer, and hydrogen m <sup>3</sup> /mole s
$T, T_f, T_{ref}$	Bed, feed and reference temperature, °C
$T_{gi}, T_g$	Temperature of recycle stream before and after cooling, °C
$T_{wi}, T_{wo}$	Cooling water temperature before and after cooling, °C
$t$	Time, s
$UA$	Overall heat transfer coefficient multiplied by the heat transfer area, cal/s K
$V_g$	Gas holdup in the reactor, m <sup>3</sup>
$x$	Vector of states
$x_{M1}, x_{M2}, x_N, x_H$	Mole fraction of monomer, co-monomer, nitrogen and hydrogen.
$X$	Hydrogen to monomer ratio
$Y, Y_p$	Vector of future outputs over $n$ and $P$ , respectively.
$Y_c$	Number of moles of catalyst site, mole
$y, y_p$	Vector of model outputs, and of plant outputs
$y_j, y_j^d$	Cumulative and instantaneous molecular weight distribution

### Greek letters

$\Delta u$	Vector of manipulated variables
$\Delta U$	Vector of M-future manipulated variables
$\Delta H_r$	Heat of reaction, cal/g
$\Lambda$	Input weight
$\Gamma$	Output weight
$\sigma$	Tuning parameter for kalman filtering
$\alpha$	Tuning parameter for the disturbance prediction model.
$\theta$	Coefficient of the disturbance prediction model

## 7. REFERENCES

- [1] J.P. Congalidis and J.R. Richards,"Process control of polymerization reactors: An industrial perspective", *Polymer Reaction Engineering*, Vol. 6, pp. 71-111, 1998.
- [2] C. Sayer, G. Arzamendi, J.M. Asua, E.L. Lima, and J.C. Pinto,"Dynamic Optimization of Semicontinuous Emulsion Copolymerization Reactions: Composition and Molecular Weight Distribution", *Computers and Chemical Engineering*, Vol. 25, pp. 839-849, 2001.
- [3] H.K. Choi and W.H. Ray,"Polymerization of Olefins through Heterogeneous Catalysis. II. Kinetics of Gas Phase Propylene Polymerization with Ziegler-Natta Catalysts", *Journal of Applied Polymer Science*, Vol. 30, pp. 1065-1081, 1985.
- [4] K.B. McAuley, D.A. McDonald, and P.J. McLellan,"Effects of Operating Conditions on Stability of Gas-phase Polyethylene Reactors", *AIChE*, Vol. 41, pp. 868-879, 1995.
- [5] K.B. McAuley and J.F. MacGregor,"Nonlinear Product Property Control in Industrial Gas-Phase Polyethylene Reactors", *AIChE Journal*, Vol. 39, pp. 855-866, 1993.
- [6] S.A. Dadebo, M.L. Bell, P.J. McLellan, and K.B. McAuley,"Temperature Control of Industrial Gas Phase Polyethylene Reactors", *J. of process control*, Vol. 7, pp. 83-95, 1997.
- [7] E.M. Ali, A.E. Abasaeed, and S.M. Al-Zahrani,"Optimization and Control of Industrial Gas-Phase Ethylene Polymerization Reactors", *Industrial and Engineering Chemistry Research*, Vol. 37, pp. 3414-3423, 1998.
- [8] H. Seki, M. Ogawa, and M. Ohshima,"PID Temperature Control of an Unstable Gas-Phase Polyolefin Reactor", *Journal of Chemical Engineering of Japan*, Vol. 34, pp. 1415-1422, 2001.
- [9] Y. Wang, H. Seki, S. Ohyama, K. Aksumatsu, M. Ogawa, and M. Ohshima,"Optimal Grade Transition Control for Polymerization Reactors", *Computers and Chemical Engineering*, Vol. 24, pp. 1555-1561, 2000.
- [10] D. Bonvin, L. Bodizs, and B. Srinivasan,"Optimal Grade Transition for Polyethylene Reactors via NCO Tracking", *Chemical Engineering Research and Design*, Vol. 83, pp. 692-697, 2005.
- [11] A.M. Cervantes, S. Tonelli, A. Brandolin, A. Bandoni, and L.T. Biegler,"Large-Scale Dynamic Optimization of a Low Density Polyethylene Plant", *Computers and Chemical Engineering*, Vol. 24, pp. 983-989, 2000.

- [12] C. Chatzidoukas, J.D. Perkins, E.N. Pistikopoulos, and C. Kiparssides, "Optimal Grade Transition and Selection of Closed-loop Controllers in a Gas-phase Olefin Polymerization Fluidized Bed Reactor", *Chemical Engineering Science*, Vol. 58, pp. 3643-3658, 2003.
- [13] D.P. Lo and W.H. Ray, "Dynamic Modeling of Polyethylene Grade Transitions in Fluidized bed Reactors Employing Nickel-Diimine Catalysts", *Industrial and Engineering Chemistry Research*, Vol. 45, pp. 993-1008, 2006.
- [14] M. Ohshima and M. Tanigaki, "Quality control of polymer production process", *J. of process control*, Vol., pp. 135-148, 2000.
- [15] C. Sato, Tetsuya Ohtani, and N. Hirokazu, "Modeling, simulation and nonlinear control of a gas-phase polymerization process", *Computers and Chemical Engineering*, Vol. 24, pp. 945-951, 2000.
- [16] G.R. Meira, "Forced Oscillations in Continuous Polymerization Reactors and Molecular Weight Distribution Control. A Survey", *Journal of Macromolecular Science-Reviews in Macromolecular Chemistry*, Vol. 20, pp. 207-241, 1981.
- [17] K. Heiland and W. kaminsky, "Comparison of Zirconocene and Hafnocene Catalysts for the Polymerization of Ethylene and 1-Butene", *Makromolekulare Chemie-Macromolecular Chemistry and Physics*, Vol. 193, pp. 601-610, 1992.
- [18] D. Beigzadeh, J.B.P. Soares, and A. Hamielec, "Recipes for Synthesizing Polyolefins with Tailor-Made Molecular Weight, Polydispersity Index, Long-Chain Branching Frequencies, and Chemical Composition Using Combined Metallocene Catalyst Systems in a CSTR at Steady State", *Journal of Applied Polymer Science*, Vol. 71, pp. 1753-1770, 1998.
- [19] L. D'Agnillo, J.B.P. Soares, and A. Penlidis, "A Critical Examination of Polyethylene Molecular Weight Distribution Control Through the Combination of Soluble Metallocene/methylalumoxane Catalysts", *polymer International*, Vol. 47, pp. 351-360, 1998.
- [20] J.D. Kim, J.B.P. Soares, and G.L. Rempel, "Use of Hydrogen for Tailoring of the Molecular Weight Distribution of Polyethylene in a Bimetallic Supported Metallocene Catalyst System." *Macromolecular Rapid Communications*, Vol. 19, pp. 197-199, 1998.
- [21] D.R. Loveday and D.H. McConville, *Mixed Catalyst Compounds, Catalyst System and Their Use in a Polymerization Process*. 2001.
- [22] H.S. Cho, J.S. Chung, and W.Y. Lee, "Control of Molecular Weight Distribution for Polyethylene Catalyzed over Ziegler-Natta /Metallocene Hybrid and Mixed Catalysts", *J. of Molecular Catalysis A: Chemical*, Vol. 159, pp. 203-213, 2000.

- [23] T.E. Nowlin, S.D. Schregenberger, P.P. Shirodkar, and G.O. Tsien, *Process for Controlling the MWD of a Broad or Bimodal resin in a Single Reactor*. 2002: USA.
- [24] E.S. Shamshoum, H. Chen, and L. Margarito, *Ziegler-Natta Catalyst with Metallocene for Olefin Polymerization*. 2003: USA.
- [25] J.B.P. Soares and A. Penlidis, "Measurement, Mathematical Modeling and Control of Distribution of Molecular Weight, Chemical Composition and Long-Chain Branching of Polyolefins Made with Metallocene Catalysts", in *Metallocene-Based Polyolefins: Preparation, Properties and Technology* J. Scheirs and W. Kaminsky, Editors Johan Wiley. 2000.
- [26] G. Debras and J. Dath, *Production of Polyethylene Having A Bimodal Molecular Weight Distribution*. 2001, Fina Research, S. A., Feluy: USA.
- [27] R.S. Schiffino, *Process for Polyolefin Production using Short Residence Time Reactors*. 1995: USA.
- [28] K.B. McAuley, J.F. MacGregor, and A. Hamielec, "A Kinetic Model for Industrial Gas-Phase Ethylene Copolymerization", *AIChE Journal*, Vol. 36, pp. 837-850, 1990.
- [29] E.M. Ali and E. Zafiriou, "Optimization-based Tuning of Non-linear Model Predictive Control with State Estimation", *J. of Process Control*, Vol. 3, pp. 97-107, 1993.